Monte Carlo simulation of ICRF discharge initiation in ITER

M. Tripský, T. Wauters, A. Lyssoivan, A. Křivská, F. Louche, M. Van Schoor, and J.-M. Noterdaeme

Citation: AIP Conference Proceedings **1689**, 060009 (2015);

View online: https://doi.org/10.1063/1.4936507

View Table of Contents: http://aip.scitation.org/toc/apc/1689/1

Published by the American Institute of Physics

Monte Carlo simulation of ICRF discharge initiation in ITER

M. Tripský[*,†,a)], T. Wauters[*], A. Lyssoivan[*], A. Křivská[*], F. Louche[*], M. Van Schoor[*] and J.-M. Noterdaeme[†]

[*]*Laboratory for Plasma Physics, ERM/KMS, 1000 Brussels, Belgium, TEC partner*
[†]*Ghent University, Department of Applied Physics, 9000 Ghent, Belgium*

[a)]Corresponding author: m.tripsky@gmail.com

Abstract. Discharges produced and sustained by ion cyclotron range of frequency (ICRF) waves in absence of plasma current will be used on ITER for (ion cyclotron-) wall conditioning (ICWC). The here presented simulations aim at ensuring that the ITER ICRH&CD system can be safely employed for ICWC and at finding optimal parameters to initiate the plasma.

The 1D Monte Carlo code `RFdinity1D3V` was developed to simulate ICRF discharge initiation. The code traces the electron motion along one toroidal magnetic field line, accelerated by the RF field in front of the ICRF antenna. Electron collisions in the calculations are handled by a Monte Carlo procedure taking into account their energies and the related electron collision cross sections for collisions with H_2, H_2^+ and H^+. The code also includes Coulomb collisions between electrons and ions ($e-e, e-H_2^+, e-H^+$).

We study the electron multiplication rate as a function of the RF discharge parameters (i) antenna input power (0.1-5MW), and (ii) the neutral pressure (H_2) for two antenna phasing (monopole [0000]-phasing and small dipole [$0\pi0\pi$]-phasing). Furthermore, we investigate the electron multiplication rate dependency on the distance from the antenna straps. This radial dependency results from the decreasing electric amplitude and field smoothening with increasing distance from the antenna straps.

The numerical plasma breakdown definition used in the code corresponds to the moment when a critical electron density n_{ec} for the low hybrid resonance ($\omega = \omega_{LHR}$) is reached. This numerical definition was previously found in qualitative agreement with experimental breakdown times obtained from the literature and from experiments on the ASDEX Upgrade and TEXTOR.

INTRODUCTION

One of the research challenges for ITER is developing effective wall conditioning techniques applicable in presence of the permanent toroidal magnetic field for (i) reducing the in-vessel impurity content, (ii) controlling the surface hydrogen isotopic ratio and (iii) mitigating the in-vessel long-term tritium inventory build-up. Present fusion machines use standardly glow discharge conditioning (GDC). This technique however cannot work in the presence of a magnetic field. Therefore discharges produced and sustained by ion cyclotron range of frequency (ICRF) waves in absence of plasma current will be used on ITER for (ion cyclotron-) wall conditioning (ICWC). The successes of this technique were demonstrated in tokamaks [1, 2] and stellarators [2].

The plasma initiation by ICRF has been studied using single particle descriptions and basic analytic models [3]. To further improve the present understanding on plasma production employing the vacuum RF field of ICRF antennas and its parametric dependencies, the Monte Carlo code **`RFdinity1D3V`** was developed in **`C++`** using standard message-passing parallel programming for run-time optimization [4]. The code runs on the HELIOS supercomputer system at Computational Simulation Centre of International Fusion Energy Research Centre (IFERC-CSC), Aomori, Japan.

The main purpose of the model is to study discharge initiation and to optimize the antenna parameters to swiftly initiate the discharge minimising the time interval with high voltage on the antenna and poor absorption of RF power.

DESCRIPTION OF MODEL `RFDINITY1D3V`

The model follows the motion of electrons around the torus along one magnetic field line accelerated only by the parallel component of the vacuum RF field in front of the ICRF antenna. Depending on their cross sections related to individual velocities of the electrons and densities of the target species, they may collide with a hydrogen molecule (H_2) or hydrogen ions (H_2^+ or H^+) according to the Monte Carlo collisions schema (***MCCS***). The cross section of the included collisions (see Table 1) are taken from [5]. Above electron densities of $n_e \geq 10^{13}\mathrm{m}^{-3}$ Coulomb collisions become important and are included according to the Takizuke-Abe (TA)-method [6]. The simulations can reach the

Radio Frequency Power in Plasmas
AIP Conf. Proc. 1689, 060009-1–060009-4; doi: 10.1063/1.4936507

TABLE 1. Summary of the included collisional reactions and Coulomb collisions in hydrogen.

	Electron collisions with H_2		**Electron collisions with H_2^+ and H^+**	**Coulomb collisions**
Ioniz.	$e+H_2 \longrightarrow e+H_2^+ +e$	Ioniz.	$e+H_2^+ \longrightarrow e+H^+ +H^+ +e$	$e+e,\ e+H_2^+,\ e+H^+$
Excit	$e+H_2 \longrightarrow e+H_2^\star$	Dissoc.	$e+H_2^+ \longrightarrow e+H^+ +H$	
Dissoc.	$e+H_2 \longrightarrow e+H+H$	Dis. Recomb.	$e+H_2^+ \longrightarrow H+H^\star$	
Dis. ioniz.	$e+H_2 \longrightarrow e+H^+ +H+e$	Recomb.	$e+H^+ \longrightarrow H+h\nu$	

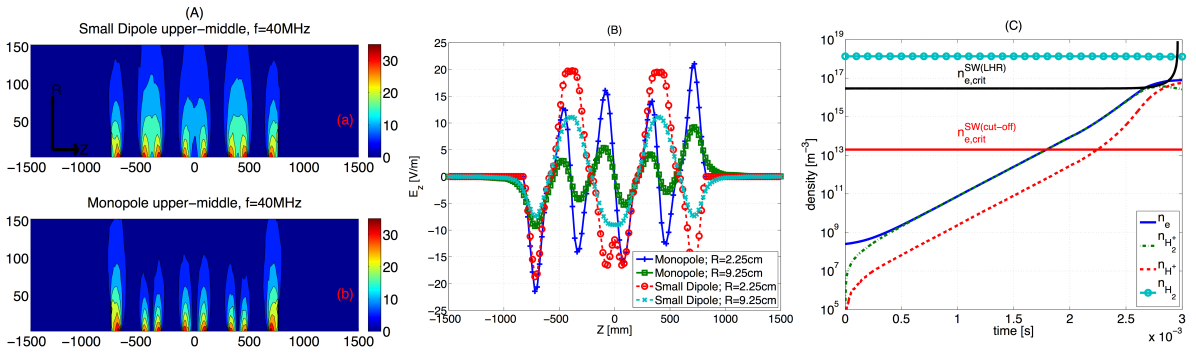

FIGURE 1. (A) Contour plot of the absolute value of the E_z-field in $(R-Z)$-coordinates simulated with the MWS code for four-strap ITER antenna in mid-upper plane, r is relative distance from antenna strap (f = 40 MHz, $P = 0.5$W): (a) Small dipole $[0\,\pi\,0\,\pi]$-phasing, (b) Monopole $[0\,0\,0\,0]$-phasing; (B) E_z-field in Monopole and Small dipole phasing at $r = 2.25$cm or $r = 9.25$cm used in the model; (C) Density evolution of species $(n_e, n_{H_2^+}, n_{H^+}, n_{H_2})$ in time.

electron densities high enough for Slow wave excitation (SW) and Fast wave excitation (FW). However, at present waves phenomena are neglected in the simulations, as well as any perturbations of the vacuum RF field due to increasing electron density.

The performed simulations use the parallel electric field profiles as obtained by 3D Microwave Studio (***MWS*** [7]) computations for the current design of the ITER antenna without Faraday screen (4 columns of straps in the toroidal direction, each column consisting of 2 poloidal triplets of straps fed in parallel by one transmission line per triplet). The results in this contribution are restricted to electric fields in two horizontal planes located in the top of the antenna and in the center of the upper half of the antenna. Figure 1(A) shows the absolute values of the E_z-field in $(r-Z)$-coordinates for two different toroidal antenna strap phasings in mid-upper-plane: (a) Small dipole (**SmD**), (b) Monopole (**M**). Figure 1(B) takes a closer look at the electric fields at two distances from the antenna strap ($r = 2.25$cm and $r = 9.25$cm) and for two antenna-phasings (***M*** and ***SmD***). The figures demonstrate that not only the amplitude of the electric field changes radially but also the shape.

Figure 1(C) shows an example of a simulated density increase of the different plasma species, where as well the threshold densities for (*Slow wave excitation*) $n_{e,crit}^{SW(cut-off)}$ and (*Lower Hybrid Resonance*) $n_{e,crit}^{SW(LHR)}$ are indicated. It is expected that upon reaching $n_{e,crit}^{SW(cut-off)}$, a first principle validity limit of the code, the $E_\parallel$ field will diverge from the vacuum field used in our model. On approaching the LHR, where $E_\parallel$ becomes very strong the vacuum field certainly cannot be used further and simulation results beyond this density with the present code version are not valid. The numerical definition of the breakdown momentum, based on RF wave physics [8], was nevertheless put at the upper validity limit $n_{e,crit}^{SW(LHR)}$.

SIMULATION RESULTS

Pressure dependency for SmD and M-phasing

A dependency of the breakdown time (t_{bkdn}) on the neutral pressure (p_{H_2}) was studied at ITER relevant ICWC pressure interval ($5\cdot10^{-3} - 1\cdot10^{-2}$Pa) at the constant antenna power $P = 5$MW and the frequency $f = 40$MHz.

Figure 2(A) illustrates the dependency of the t_{bkdn} on the radial distance from the antenna in the mid-upper plane for two pressures and for the **M** and **SmD**-phasing. The breakdown time t_{bkdn} clearly is lower for higher neutral pressures p_{H_2} at a same radial distance from the antenna. The dependency on the radial distance is related to the varying shape of the E_z and decreasing amplitude when moving away from the antenna strap. The figure shows that the most effective

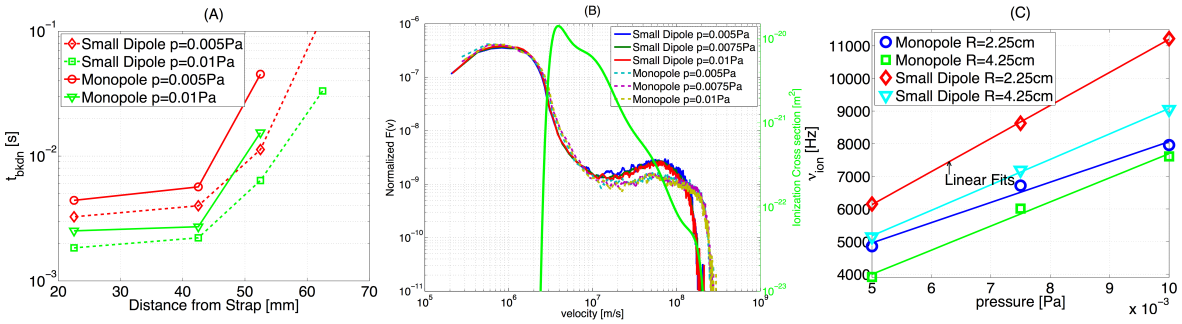

FIGURE 2. (A) The breakdown time t_{bkdn} radial dependency with the varying neutral pressure for **M** and **SmD**-phasing in mid-upper plane; (B) Velocity distribution for varying pressure p_1, p_2 and p_3 for one radial distance $r = 4.25$cm and for two antenna phasings **M** and **SmD**; (C) Linear dependency of ionization frequency ν_{ion} on the neutral pressure at two radial distances: $r = 2.25$cm and $r = 4.25$cm for **M** and **SmD**-phasing.

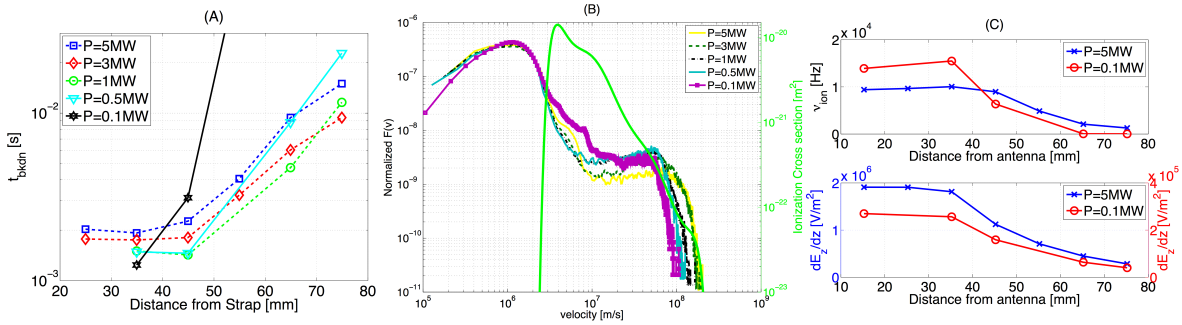

FIGURE 3. (A) The breakdown time t_{bkdn} radial dependency with the varying antenna power for **SmD**-phasing in top plane; (B) Velocity distribution for varying antenna power $P = [5, 3, 1, 0.5, 0.1]$MW at radial distance $r = 3.5$cm with **SmD**-phasing; (C) Dependencies of the function ν_{ion} and dE_z/dz on the radial distance at $P = 5$MW and $P = 0.1$MW.

area for the discharge initiate is below 50mm. Furthermore the t_{bkdn} is constant in this area.

For these simulations it is found that the varying pressure has little effect on the shape of the velocity distribution. Figure 2(B) shows the velocity distributions with varying pressure and for the **M** and **SmD**-phasing, together with the ionization cross section. The distributions for **M** and **SmD** are slightly different: (i) unlike the **SmD**, the **M** distributions extend wider to velocities that do not contribute anymore to ionization, (ii) for **SmD**, between velocities of 10^7m/s and 10^8m/s, the distribution is two times larger than for **M**. These small differences result in a slightly faster breakdown for **SmD** than for **M** in our simulations. However this may be in discrepancy with the experiment as observations on e.g. tokomaks TORE SUPRA or TEXTOR where the monopole-phasing is more effective for plasma initiation than dipole-phasing [9].

The ionization frequency can be expressed as $\nu_{ion} = n_{H_2}\langle\sigma(v)v\rangle^{ion}_{e,H_2}$, where $\langle\sigma(v)v\rangle^{ion}_{e,H_2}$ is the ionization reaction rate determined by the electron velocity distribution. As the velocity distributions for the studied pressure interval have almost the same shape, the ionization frequency depends solely on the neutral pressure. The Figure 2(C) demonstrates the linear dependency of ν_{ion} on the neutral pressure p_{H_2} for two radial distances and for **M** and **SmD**-phasing.

Power dependency for SmD

The power scan was performed in the top-plane at $f = 40$MHz and $p_{H_2} = 1 \cdot 10^{-2}$Pa for the **SmD**-phasing. The vacuum electric field strength is determined by the input power as well as by the distance from the antenna straps. Results of the breakdown time dependency on the antenna power are illustrated in Figure 3(A). We observed that at the relative distances below 50mm from the antenna strap the breakdown time (t_{bkdn}) does not change dramatically with the varying antenna power ($P = 0.5 - 5$MW) and the value of the t_{bkdn} lay between 1ms and 2.5ms. Simulations for the lowest power $P = 0.1$MW have also the lowest t_{bkdn} but only relatively close to the straps. Above 40mm the t_{bkdn} for this power becomes larger than for the simulations with higher power. For the higher power also, the breakdown time increases above 50mm, due to decaying electric field and the smoothening of the electric field profiles.

Figure 3(B) illustrates the velocity distribution $F(v)$ during plasma production taken at $r = 35$mm for the different antenna powers, together with the ionization cross section. For the shown distributions $F(v)$, the one at

$P = 0.1$MW has the largest electron population at the interval where the ionization cross section is the most significant, $v = \left(3 \cdot 10^6 - 1 \cdot 10^7\right)$m/s, while the width of the distribution increases with increasing power. The depopulation of electrons from the velocity interval relevant for ionization reactions results in longer breakdown times at higher input power.

Figure 3(C) shows the ionization frequency as a function of the radial position and gradient of the E_z-field (dE_z/dz) at the edge of the antenna box in the top-plane (see Figure 1(A-B) at $Z = 750$mm) as a function of the radial position for two antenna powers $P = 5$MW and $P = 0.1$MW. Although the electric field amplitudes at 0.1MW is seven times lower than for 5MW, we recognize a similar shape for the ionization frequency: about constant below $r = 50$mm and gradually decaying towards larger distances. This tendency is correlated with the dE_z/dz, which is found to be a measure for low energy electrons to gain energy in the oscillating electric field when approaching the antenna area.

CONCLUSION

First results of the code `RFdinity1D3V` with the ITER ICRF antenna parallel electric field E_z for simulating the initial breakdown phase for magnetised toroidal ICRF discharges were presented. The simulations learn that on ITER ICRF plasma can be produced at modest ($P = 0.5$MW) to high ($P = 5$MW) RF power levels and for typical ICWC pressure levels of $5 \cdot 10^{-3} - 1 \cdot 10^{-2}$Pa.

The model allows to study the electron velocity distribution as a function of the ICRF discharge parameters: electric field shape and amplitude, antenna input power, RF frequency, neutral hydrogen pressure, antenna phasing and both radial and vertical position. The shape of the velocity distribution during plasma production determines, via the velocity dependent ionization cross section, the rate ν_{ion} at which the electron density increases.

The linear dependency of the ν_{ion} on the neutral hydrogen pressure within the supposed ITER ICWC pressure range ($5 \cdot 10^{-3}$Pa $- \ 1 \cdot 10^{-2}$Pa) was demonstrated due to an almost identical shape of the velocity distribution. Due to the radial decreasing E_z-field amplitude and changing shape, the most efficient area for the plasma initiation lies at distances below 50mm from the antenna straps for both the studied top and the mid-upper planes. Also within this radial distance the breakdown time is about constant. Above this radial distance the t_{bkdn} starts to increase due to the smoothening of the E_z-field and its decreasing amplitude. It is observed that the simulations with modest antenna power ($P \leq 1$MW) show more effective plasma initiation due to better overlap of the velocity distribution and ionization cross section than at the higher antenna power.

The simulations for **SmD**-phasing had shorter breakdown times than the simulations for **M**-phasing. As this result is in discrepancy with experimental observations on present tokamaks it requires further investigation. The frequency dependency will be subject of a future publication.

Acknowledgements

This work was carried out using the HELIOS supercomputer system at Computational Simulation Centre of International Fusion Energy Research Centre (IFERC-CSC), Aomori, Japan, under the Broader Approach collaboration between Euratom and Japan, implemented by Fusion for Energy and JAEA. This work has been carried out within the framework of the EUROfusion Consortium and has received funding from the Euratom research and training programme 2014-2018 under grant agreement No 633053. The views and opinions expressed herein do not necessarily reflect those of the European Commission.

REFERENCES

1. A. Lyssoivan, *J. Nucl. Mater.* **456**, 337–339 (2005).
2. T. Wauters, and H. P. Laqua, *AIP Conference Proceedings* **415** (2014).
3. A. Lyssoivan, and D. Douai, *Plasma Phys. Control. Fusion* **54** (2012).
4. M. Tripsky, and T. Wauters, "Monte Carlo simulation of ICRF discharge initiation at $\omega_{LHR} < \omega$," in *European Conference Abstracts*, European Conference Abstracts (ECA), 2014, vol. 38F.
5. D. Reiter, The data file HYDHEL, Atomic and Molecular Data for EIRENE, Tech. rep., Fz-Juelich GmbH (2002).
6. T. Takizuka, and H. Abe, *J. Comput. Phys.* **25** (1977).
7. CST AG, `http://www.cst.com`, CST STUDIO SUITE(R) (2015).
8. A. Lyssoivan, and T. Wauters, "Wave aspect of neutral gas breakdown with ICRF antenna in ICWC operation mode," in *European Conference Abstracts*, European Conference Abstracts (ECA), 2014, vol. 38F.
9. A. Lyssoivan, and R. Koch, *J. Nucl. Mater.* **415** (2011).